

Target dependence of intermittency and multifractality of multiplicity fluctuations in 800-GeV proton emulsion-nuclei interactions

R. K. Shivpuri and V. K. Verma

Department of Physics and Astrophysics, University of Delhi, Delhi-110007, India

(Received 10 August 1992)

The scaled factorial moments and multifractal moments were investigated for secondary particles for various targets in 800-GeV interactions with emulsion nuclei. The results show clear evidence for intermittent behavior according to the self-similar cascade mechanism. The self-similar structure is also observed from the analysis of multifractality as the spectrum of scaling indices, $f(\alpha_q)$ shows a self-similar behavior in these interactions. The self-similar multifractal structure is found to be consistent with the jet cascading mechanism. The universality of pseudorapidity distribution in interactions with various targets is found from the analysis of the rescaled spectrum function $\tilde{f}(\tilde{\alpha}_q)$. The phase transition is not indicated in our data, either from the analysis of intermittency or from the multifractal analysis.

PACS number(s): 13.85.Hd

I. INTRODUCTION

The large density fluctuations in multiparticle production in small rapidity regions at high energies possess self-similar properties [1–4] as the resolution in phase space is increased up to the experimental or statistical limit. Bialas and Peschanski [5] have called such multiplicity fluctuations intermittency which is based on the idea of the analogous bursts of turbulence in the theory of chaos [6]. It was suggested [5] that there is a power-law dependence of the scaled factorial moments of multiplicity distribution on the rapidity bin width. This intermittent behavior has been observed in various collision processes with various beams and targets at different high energies [1,3,4]. The present day models on hadronic collisions are unable to reproduce the intermittent behavior of the experimental data [1,4]. For e^+e^- annihilation, the Lund parton shower model [7] reproduces the experimental results very well [1,4] especially in the framework of the Monte Carlo code JETSET [8]. It is useful to find out the various sources that contribute to multiparticle fluctuations which characterize the dynamical process of particle production.

The scaled factorial moments are defined for positive integral orders. In order to extend to negative moments, the multifractal analysis has been proposed [9–11]. Hwa [10] has suggested an alternative set of moments G_q which is used to investigate the large density fluctuations in terms of the multifractal formalism. These moments are more direct in exploring the multiplicity fluctuations in rapidity space. Thus, if the multiplicity fluctuations in multiparticle production have a dynamical origin and not statistical, the fractal properties [12] can be used to investigate the hadronization in high-energy collisions. It is found that the spectral function $f(\alpha_q)$ characterizes the nature of fluctuations [13] for various types of reactions. Such structure has been found to be exhibited in e^+e^- annihilations [14], $\bar{p}p$ collisions [15,16], π^+p and K^+p collisions [17], and μp and μd collisions [18–20].

In this paper, we present results on intermittency in multiparticle production in proton interactions with various target nuclei in emulsion at 800 GeV, which is the highest available energy for fixed targets. The dependence of the scaled factorial moments on the shape of the single-particle pseudorapidity distribution has been corrected [21]. We have also studied the slope and the fractal dimension [9,10] of the scaled factorial moments for these targets. As predicted by QCD the existence of a phase transition [22] in the present interactions has been investigated. The multifractal analysis of the interactions has also been studied. We have studied the spectrum [10] $f(\alpha_q)$ of scaling indices which is characteristic of the nature of fluctuations taking place in these interactions. We are also presenting the results of the fractal dimension [23] of the multifractal moments, the formalism for which has been recently developed [23–27] and applied effectively in multiparticle production [10]. We have rescaled the spectral function as suggested by Chiu and Hwa [28] which is useful in looking into the form of universality that unifies the multifractal structure for positive order of moments of our analysis for different targets in emulsion. It is the universality between various types of interactions in emulsion which signifies the fractal dimensions and other generalized indices, fundamentally.

II. THE EXPERIMENT

A stack of 40 Ilford G5 emulsion pellicles of dimensions $10 \times 8 \times 0.06$ cm³ was exposed to a proton beam of energy 800 GeV at Fermilab. The beam flux was 8.7×10^4 particles/cm². The scanning of the interactions was done under 40X objective of the high-resolution microscopes by the area scanning method. Using the double scan data, the scanning efficiency was calculated for each observer and the overall efficiency was found to be $\sim 96\%$. In order to make sure that the interactions are due to beam only all the interactions were followed back.

TABLE I. The statistics for various categories of interactions in 800-GeV p -emulsion nuclei interactions, with $N_s > 10$. The errors are statistical.

Category	Number of events	$\langle N_h \rangle$	$\langle N_s \rangle$	$\langle N_s \rangle_{\Delta\eta=0.5-5.5}$
p -nucleon	212	0.32 ± 0.02	15.76 ± 1.08	14.67 ± 1.01
p CNO	393	3.52 ± 0.18	18.44 ± 0.93	17.28 ± 0.87
p -AgBr	864	16.05 ± 0.55	25.28 ± 0.86	23.69 ± 0.81

The interactions lying within $25 \mu\text{m}$ each from the air and the glass surface has not been considered for measurement purposes. Following these criteria, the total number of events selected for measurement were found to be 2318. All the measurements were done under 100X oil immersion objectives. Following the usual terminology [29], the secondary particles having $\beta(v/c) \geq 0.7$ and < 0.7 were designated as shower and heavy tracks, respectively, the multiplicities of which were designated as N_s and N_h , respectively. The angles of the shower tracks with respect to beam axis were measured by the coordinate method. The values of x , y , and z coordinates at the vertex and two points each on the shower and beam tracks were measured. The polar angle (θ) for each shower particle was calculated using the three-dimensional (3D) coordinate geometry formulation. The uncertainty in angle measurement was determined to be 8×10^{-4} rad. The basic parameter which shows the fluctuations is the rapidity (y) which is defined as

$$y = \frac{1}{2} \ln[(E + P_L)/(E - P_L)], \quad (1)$$

where E and P_L are the energy and the longitudinal momentum of the shower particles, respectively. In the

present investigation, we have used pseudorapidity (η) of the shower particles, which is given by

$$\eta = -\ln[\tan(\theta/2)] \quad (2)$$

which is a good approximation to rapidity (y) for very high energies.

It has been shown [29] that the target nucleus can be broadly identified on the basis of value of N_h as the value of N_h reflects the number of nucleons that have participated in the interaction. The interactions having $N_h \leq 1$, $2 \leq N_h \leq 5$, and $N_h \geq 9$ can be assumed to belong to nucleon, CNO, and AgBr targets, respectively. The interactions with $N_h \leq 1$ are either due to collision with pure H nuclei or due to the interactions with a single nucleon of other emulsion nuclei wherein the rest of the nucleus remains a spectator during the collision [30]. The shower particle production takes place only in the elementary proton-nucleon collision. The interactions with $2 \leq N_h \leq 5$ were considered [30] to belong mostly to proton-light nuclei (CNO) interactions. The interactions with $6 \leq N_h \leq 8$ are not considered as they could be from collisions with light nuclei as well as with heavy nuclei.

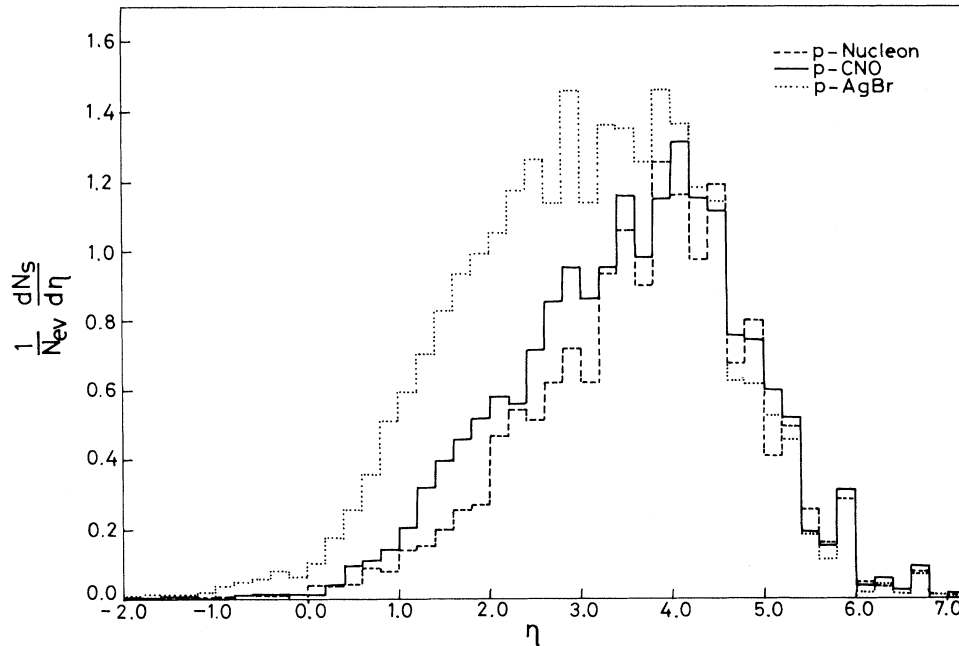


FIG. 1. Single-particle pseudorapidity distribution $\rho(\eta)$ for p -nucleon interactions (dashed lines), p -CNO interactions (solid lines), and p -AgBr interactions (dotted lines) in the laboratory frame.

The interactions with $N_h \geq 9$ are unambiguous interactions with AgBr nuclei [30].

In the present work, only the interactions with $N_s > 10$ are considered as the events with $N_s \leq 10$ have large statistical fluctuations, which might mask the dynamical effects. The density fluctuations are studied in a limited pseudorapidity range $\Delta\eta = 0.5 - 5.5$ leaving the fragmentation tails where the statistics are low. Table I shows the number of interactions for various targets with $N_s > 10$ along with the corresponding values of $\langle N_h \rangle$, $\langle N_s \rangle$, and $\langle N_s \rangle$ in $\Delta\eta$.

The single-particle pseudorapidity density is defined as

$$\rho(\eta) = \frac{1}{N_{ev}} \frac{dN_s}{d\eta}, \quad (3)$$

where N_{ev} is the number of interactions for different categories of target ("ev" denotes event). Figure 1 shows the single-particle pseudorapidity distribution for interactions with nucleon, CNO, and AgBr having $N_s > 10$ in a bin width $= 0.2$ unit/bin. The three regions, namely, target fragmentation region, central region, and projectile fragmentation region are clear from the above η distribution. It is clear that the contribution of the target fragmentation region increases with the increase in target size.

III. THE INTERMITTENCY

Consider the pseudorapidity range $\Delta\eta$ which is divided into M bins of equal width $\delta\eta = \Delta\eta/M$. Then for an ensemble of events of varying multiplicity, the q th-order scaled factorial moment is given by [5]

$$\langle F_q \rangle = \frac{1}{N_{ev}} \sum_{N_{ev}} M^{q-1} \sum_{m=1}^M \frac{k_m(k_m-1) \cdots (k_m-q+1)}{\langle N \rangle^q}, \quad (4)$$

where k_m is the number of shower particles in the m th bin for a single event and $\langle N \rangle$ is the average multiplicity in the pseudorapidity range $\Delta\eta$. The factorial moment $\langle F_q \rangle$ averaged over many events are equal to be moments of a true probability distribution of the particle density in pseudorapidity space [5]. Thus the problem of statistical fluctuations due to a finite number of particles per event is reduced.

The nonstatistical fluctuations of particle changes the absolute value of moments and also influences the variation of moments with the size of the pseudorapidity bin width $\delta\eta$. An intermittent pattern of the multiplicity fluctuation leads to a power-law behavior of the moments [5] which is given by

$$\langle F_q \rangle = [\Delta\eta/\delta\eta]^{\phi_q}, \quad 0 < \phi_q < q-1, \quad (5)$$

where ϕ_q characterizes the strength of intermittency signal. Hence, a characteristic linear rise of $\ln \langle F_q \rangle$ with $-\ln \delta\eta$ for all bin widths $\delta\eta$ down to the smallest, i.e., up to the limit of experimental resolution or the statistical limit, is predicted. The physical meaning of ϕ_q has been well explained [5] on the basis of the self-similar cascade model.

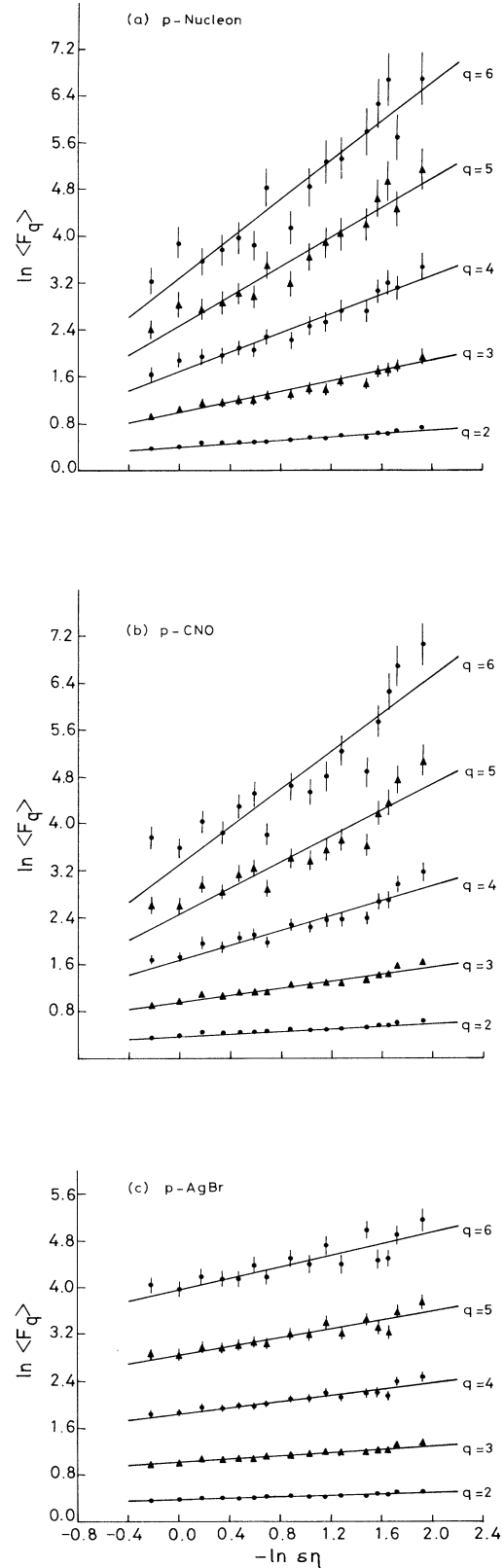


FIG. 2. $\ln \langle F_q \rangle$ as a function of $-\ln \delta\eta$ for (a) p -nucleon interactions, (b) p -CNO interactions and (c) p -AgBr interactions. The solid lines indicate the least-squares fit to the data points.

TABLE II. Values of the slopes ϕ_q obtained from least-square fits of Eq. (6) (text) to the data for the q th-order scaled factorial moments [Eq. (4) in the text] for various targets. The errors are standard.

Category	ϕ_2	ϕ_3	ϕ_4	ϕ_5	ϕ_6
p -nucleon	0.140 ± 0.012	0.422 ± 0.033	0.825 ± 0.059	1.278 ± 0.103	1.689 ± 0.170
p -CNO	0.111 ± 0.008	0.304 ± 0.025	0.642 ± 0.061	1.119 ± 0.122	1.624 ± 0.199
p -AgBr	0.070 ± 0.006	0.163 ± 0.014	0.266 ± 0.027	0.372 ± 0.048	0.489 ± 0.081

The scaled factorial moments $\langle F_q \rangle$ with $q=2-6$ are calculated according to Eq. (4) for interactions with nucleon, CNO, and AgBr targets. Figures 2(a)–2(c) show $\ln \langle F_q \rangle$ as a function of $-\ln \delta \eta$ for interactions with nucleon, CNO, and AgBr targets, respectively. The values of $\ln \langle F_q \rangle$ for interactions with nucleon and CNO targets are almost equal and much larger than those for interactions with AgBr targets. This is due to the presence of more low multiplicity interactions with nucleon and CNO targets than with AgBr targets. In these figures the errors shown are statistical. The error bars for interactions with nucleon and CNO targets are large which is due to low statistics. The distribution for high orders of moments exhibit an irregular behavior more in interactions with nucleon and CNO targets than in the AgBr targets. In all the three cases, a linear rise of moments

with decreasing bin width $\delta \eta$ is observed and thus we conclude that indeed an intermittent behavior is being observed in all the three classes of interactions. The slope ϕ_q , a characteristic parameter of the intermittency, is obtained by fitting the data points to the relation

$$\ln \langle F_q \rangle = A - \phi_q \ln \delta \eta, \quad (6)$$

where A is a constant. The region of fit in all the three figures is for $-\ln \delta \eta = 0.00-1.92$. The solid line in Figs. 2(a)–2(c) denotes the least-squares fit to the data. Table II shows the values of the slopes for interactions with nucleon, CNO, and AgBr targets. Thus, it is found that with the increase in target mass, the slope decreases for each order of moments.

The scaling behavior of factorial moments has been correlated [9] to the physics of fractal objects (particle emission sources) through the anomalous fractal dimension d_q which can be computed directly from the fitted slopes ϕ_q by the relation [10]

$$d_q = \phi_q / (q - 1). \quad (7)$$

Figure 3 shows the values of d_q versus order (q) of the

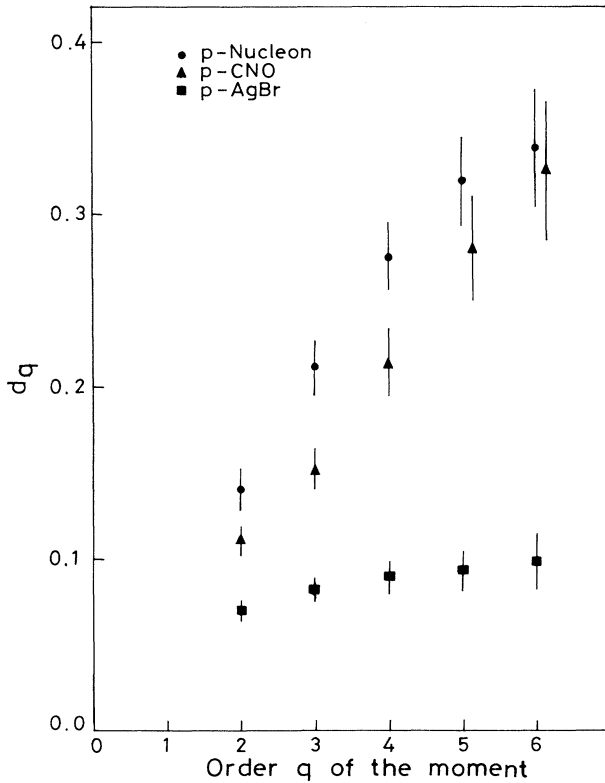


FIG. 3. The anomalous fractal dimension d_q as a function of q (order of the moments) for p -nucleon interactions [circles], p -CNO interactions [triangles], and p -AgBr interactions [squares] for the scaled factorial moments.

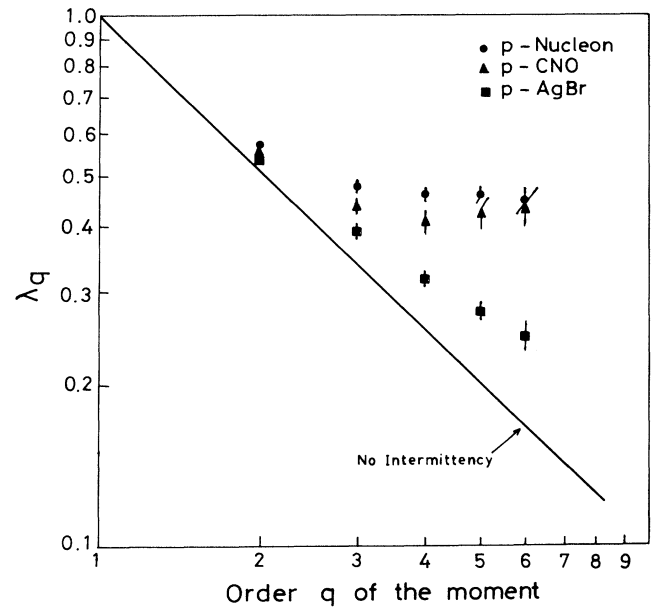


FIG. 4. λ_q as a function of q (order of the moments) for p -nucleon interactions [circles], p -CNO interactions [triangles], and p -AgBr interactions [squares] for the scaled factorial moments.

moments for interactions with nucleon, CNO, and AgBr targets. The errors shown are standard errors. It is clear from Fig. 3 that as target mass increases, the dimension d_q decreases for each order of moments. The observed behavior of dimension d_q is suggestive of a self-similar cascade mechanism for interactions with nucleon, CNO, and AgBr targets. Similar behavior is also found in lepton-hadron and hadron-hadron interactions [31].

Peschanski [22] suggested a theoretical relation between intermittency, random-cascading model, and statistical mechanics of systems with disorder such as a spin-glass phase. Such a system leads to nonthermal phase transition and if such a nonthermal phase is present, then the function [32]

$$\lambda_q = (\phi_q + 1)/q \quad (8)$$

should have a minimum at a certain value of $q = q_c$ and cannot have a maximum in the region $q \geq 1$. Here, λ_q plays the role of a (generalized) free-energy density and q

plays the role of inverse temperature. Figure 4 shows the variation of λ_q as a function of q for interactions with nucleon, CNO, and AgBr targets. The errors shown are standard errors. The solid line indicates the nonexistence of intermittency. The data points of our investigation for interactions with nucleon, CNO, and AgBr targets deviate from this solid line which indicates the presence of intermittency. For the CNO data, the low value of λ_q at $q = 4$ is not statistically different (within 1 standard deviation) than the values of λ_q at $q = 5$ and 6. Thus no minimum is clearly discernible from the CNO distribution. Further, the minimum value of λ_q for a certain value of $q = q_c$ is not obtained for the nucleon and AgBr data as well. Hence the presence of nonthermal phase transition is not clearly indicated. Similar deviations are found for data from NA22 and KLM collaborations [32].

In order to take account of the nonuniform shape of the single-particle pseudorapidity distribution, it was suggested by Fialkowski, Wosiek, and Wosiek [21] that the factorial moments can be corrected by including a factor R_q given by

$$R_q(\delta\eta) = \frac{1}{M} \sum_{m=1}^M \left[\frac{1}{\delta_m} \int_{\delta_m} \rho(\eta) d\eta \right]^q / \left[\frac{1}{\Delta\eta} \int_{\Delta\eta} \rho(\eta) d\eta \right]^q, \quad (9)$$

where δ_m denotes the m th pseudorapidity bin. The q th-order scaled factorial moment is, then, corrected as

$$\langle F_q \rangle_{\text{corr}} = \langle F_q \rangle / R_q. \quad (10)$$

From Fig. 1, it is clear that $\rho(\eta)$ distribution is not flat for the pseudorapidity range $\Delta\eta = 0.5 - 5.5$ for interactions with nucleon, CNO, and AgBr targets and hence the correction factor R_q plays an important role.

Figures 5(a)–5(c) show the value of $\ln \langle F_q \rangle_{\text{corr}}$ as a function of $-\ln \delta\eta$. The errors shown here are statistical. It is clear from these three figures that as the interacting targets becomes heavier, the variation of $\ln \langle F_q \rangle_{\text{corr}}$ for a range of $\delta\eta$ becomes less irregular for each order of moments. The regions of fit in all the three figures are the same as considered in Figs. 2(a)–2(c). The slopes ϕ_q are obtained by least-squares fit of Eq. (6) of the data points. The solid lines are the least-squares fit to the data points for each order of moments for interactions with nucleon, CNO, and AgBr targets. The slope ϕ_q thus obtained are listed in Table III and it is found that even after the corrections, ϕ_q (nucleon targets) $> \phi_q$ (CNO targets) $> \phi_q$ (AgBr targets) for each order of moments. The anomalous fractal dimension d_q [9,10] are computed using Eq. (7) and are shown in Fig. 6 for interactions with nucleon, CNO, and AgBr targets. The observed pattern of d_q is suggestive of a self-similar cascade mechanism [31]. Even after the corrections, it is found that d_q (nucleon targets) $> d_q$ (CNO targets) $> d_q$ (AgBr targets). The errors shown here are standard errors. Using Eq. (8) we have calculated the values of λ_q [32] for each order of moment and are plotted in Fig. 7 as a function of q . The errors shown are standard errors. The solid line indicates

the nonexistence of intermittency and the deviation of data points of our investigation indicates the presence of intermittency for all the three types of interactions. The error bars for interactions with nucleon and CNO targets are large and hence the existence of phase transition is not clearly indicated.

IV. MULTIFRACTALITY

In order to study the multifractal structure in multiparticle production at high energy, Hwa [10] has proposed a set of moments G_q where q is the order of moment, positive or negative and real. Initially, Hwa [10] proposed the vertical analysis, but this analysis has not been applied to any model or data. Later on, Chiu and Hwa [11] proposed the horizontal analysis and applied it to the ϕ^3 and gluon models. The horizontal analysis also maximize the information on multiplicity fluctuation. This method of analysis has been applied to e^+e^- annihilation [14], $\bar{p}p$ collision [15,16] π^+p and K^+p collisions [17], and μp and μd collisions [18–20]. Here, we also consider the horizontal analysis of G_q moments.

Let the pseudorapidity range $\Delta\eta$ be divided into M bins of equal width $\delta\eta = \Delta\eta/M$. Let N be the number of shower particles in one event in pseudorapidity range $\Delta\eta$ and k_m be the number of particles in the m th bin. Then multifractal moment G_q is defined as [11]

$$G_q = \sum_{m=1}^M \left[\frac{k_m}{N} \right]^q = \sum_{m=1}^M p_m^q, \quad (11)$$

where $p_m = k_m/N$ is the probability of shower particles in m th bin for one event. Here, q is a real number and the

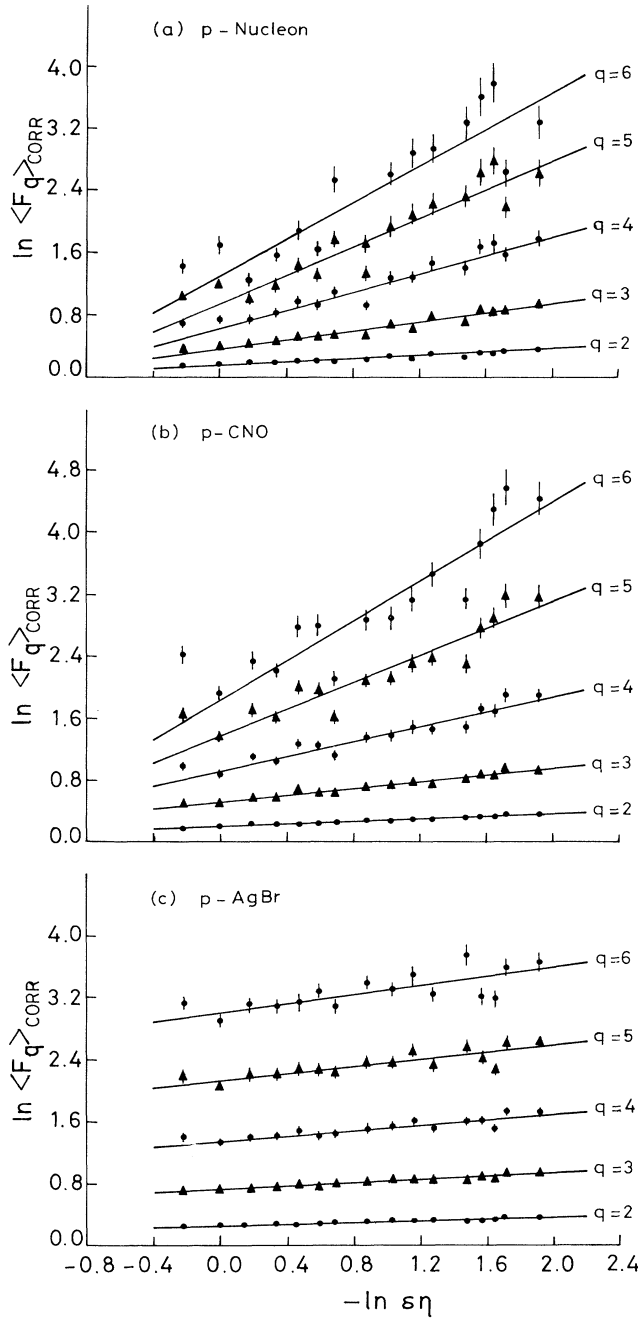


FIG. 5. $\ln \langle F_q \rangle_{\text{corr}}$ as a function of $-\ln s\eta$ for (a) p -nucleon interactions, (b) p -CNO interactions, and (c) p -AgBr interactions. The solid lines indicate the least-squares fit to the data points.

summation in Eq. (11) is carried over nonempty bins only. If multifractal structure is exhibited by the particle production process in a region of $\delta\eta$ then the moments G_q should have a power-law behavior [11] as

$$G_q \propto (\delta\eta)^\gamma(q). \quad (12)$$

The lowest limit of k_m for a nonempty bin is 1. Hence, by Eq. (11) when $\delta\eta \rightarrow 0$, G_q approaches $N^{(1-q)}$ for an event with N shower particles. Hence $\delta\eta \rightarrow 0$ limit is trivial and the power-law behavior defined in Eq. (12) does not appear for $\delta\eta \rightarrow 0$. Thus, the problem in multiparticle production is different from those in geometrical and statistical problems [33]. Hence, in order to extract the slope $\langle \Upsilon(q) \rangle$ we consider the region where M is not very large.

For an ensemble of events, Eq. (11) is applied as

$$\langle \ln G_q \rangle = \frac{1}{N_{\text{ev}}} \sum_{N_{\text{ev}}} \ln G_q, \quad (13)$$

i.e., the average of $\ln G_q$ is taken over all the events of the sample [34] and the slope, thus calculated is designated as $\langle \Upsilon(q) \rangle$.

The value of $\langle \ln G_q \rangle$ is calculated, according to Eq. (13), for the ensemble of events for q ranging from -6.0 to 6.0 . The step size is 0.5 except in the region $-1.0 < q < 1.0$ where the step size is 0.1 . Figures 8(a)–8(c) show the values of $\langle \ln G_q \rangle$ as a function of $-\ln \delta\eta$ for interactions with nucleon, CNO, and AgBr targets, respectively. In all the three figures, the values of $\langle \ln G_q \rangle$ are plotted for a few values of q as indicated in the figures in the interest of clarity. For the same reason, only some representative statistical errors are plotted in the three figures. However, the statistical errors are $\sim 7\%$ for nucleon targets [Fig. 8(a)], $\sim 5\%$ for CNO targets [Fig. 8(b)], and $\sim 3\%$ for AgBr targets [Fig. 8(c)]. The saturation behavior is observed in the large $-\ln \delta\eta$ region for low values of q ($q < 1$). Also, early saturation is observed in Fig. 8(a) (nucleon targets) than in Fig. 8(c) (AgBr targets), which is due to the presence of more low multiplicity events in interactions with nucleon targets than with AgBr targets.

The average slopes $\langle \Upsilon(q) \rangle$ are calculated by the method of least-squares fit applied to the data between $M=1$ and $M=5$.

The generalized dimension (Renyi dimension) D_q is related to the slope $\langle \Upsilon(q) \rangle$ by [24]

$$D_q = \frac{\langle \Upsilon(q) \rangle}{q-1}. \quad (14)$$

Thus, the generalized dimension D_q is calculated for the

TABLE III. Value of the slopes ϕ_q obtained from least-square fits of Eq. (6) (text) to the data for q th-order scaled factorial moment [Eq. (10) in the text] for various targets. The errors are standard.

Category	ϕ_2	ϕ_3	ϕ_4	ϕ_5	ϕ_6
p -nucleon	0.093 ± 0.008	0.295 ± 0.020	0.593 ± 0.044	0.918 ± 0.097	1.184 ± 0.178
p -CNO	0.077 ± 0.004	0.216 ± 0.015	0.483 ± 0.040	0.875 ± 0.087	1.281 ± 0.153
p -AgBr	0.046 ± 0.003	0.108 ± 0.009	0.171 ± 0.021	0.230 ± 0.041	0.291 ± 0.073

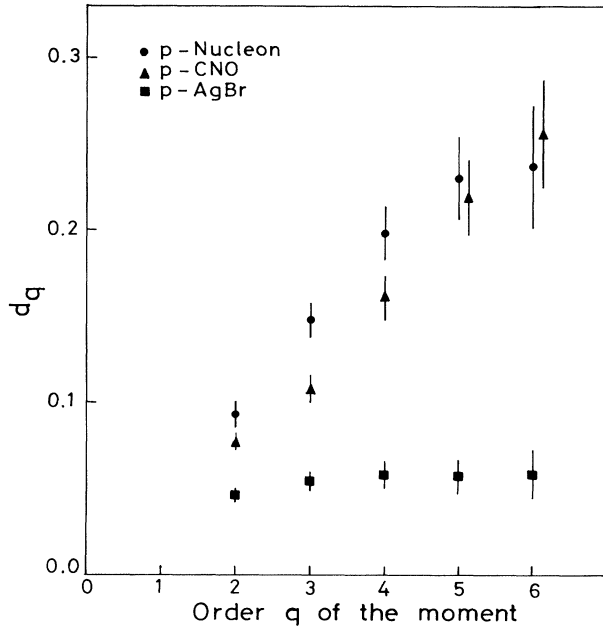


FIG. 6. The anomalous fractal dimension d_q as a function of q (order of the moments) for p -nucleon interactions [circles], p -CNO interactions [triangles], and p -AgBr interactions [squares] for the corrected scaled factorial moments.

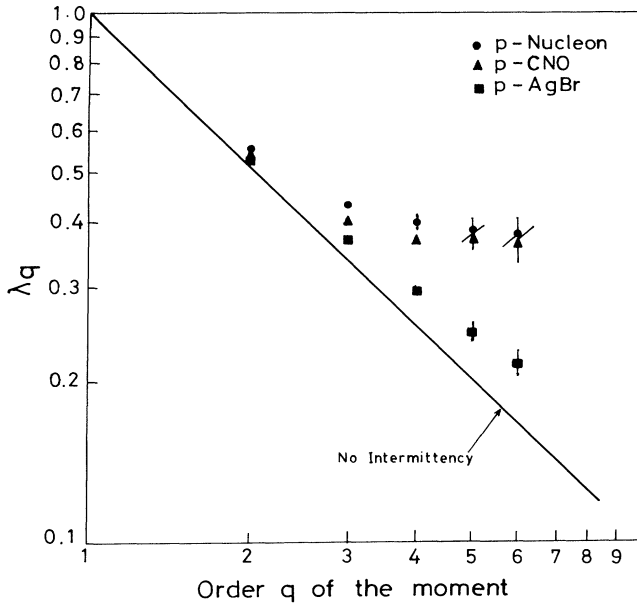


FIG. 7. λ_q as a function of q (order of the moments) for p -nucleon interactions [circles], p -CNO interactions [triangles], and p -AgBr interactions [squares] for the corrected scaled factorial moments.

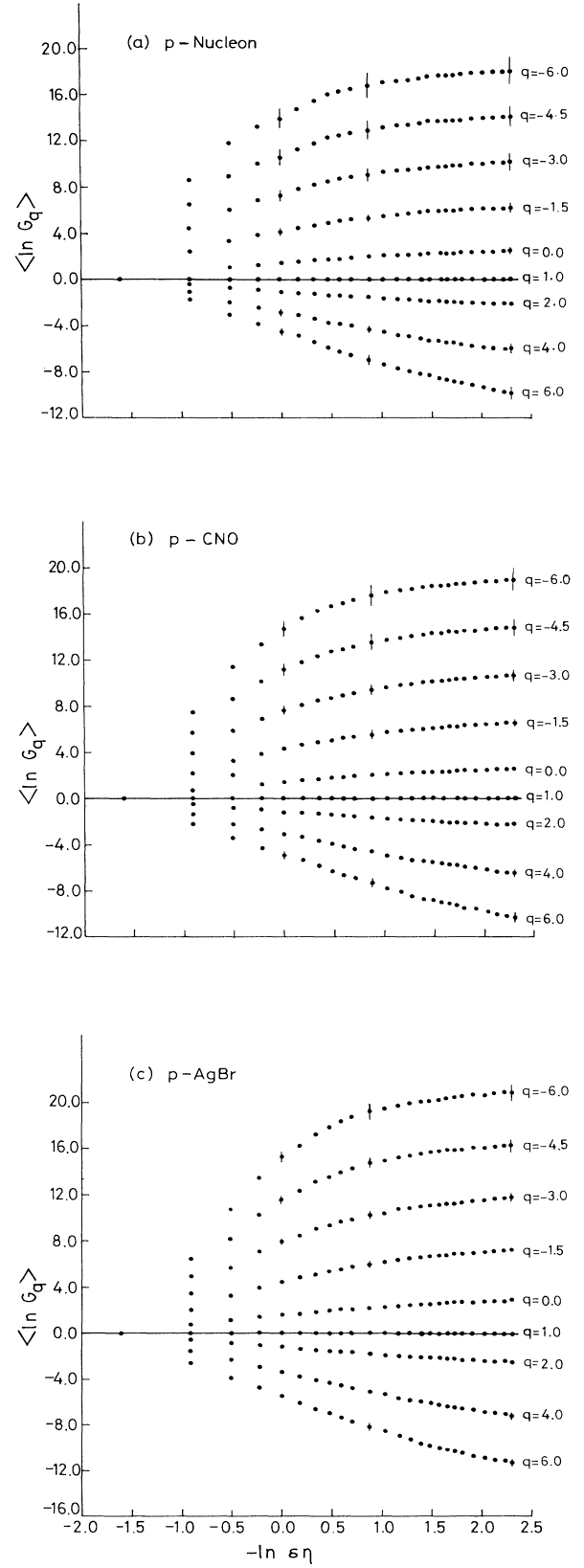


FIG. 8. $\langle \ln G_q \rangle$ as a function of $-\ln \delta \eta$ for (a) p -nucleon interactions, (b) p -CNO interactions, and (c) p -AgBr interactions.

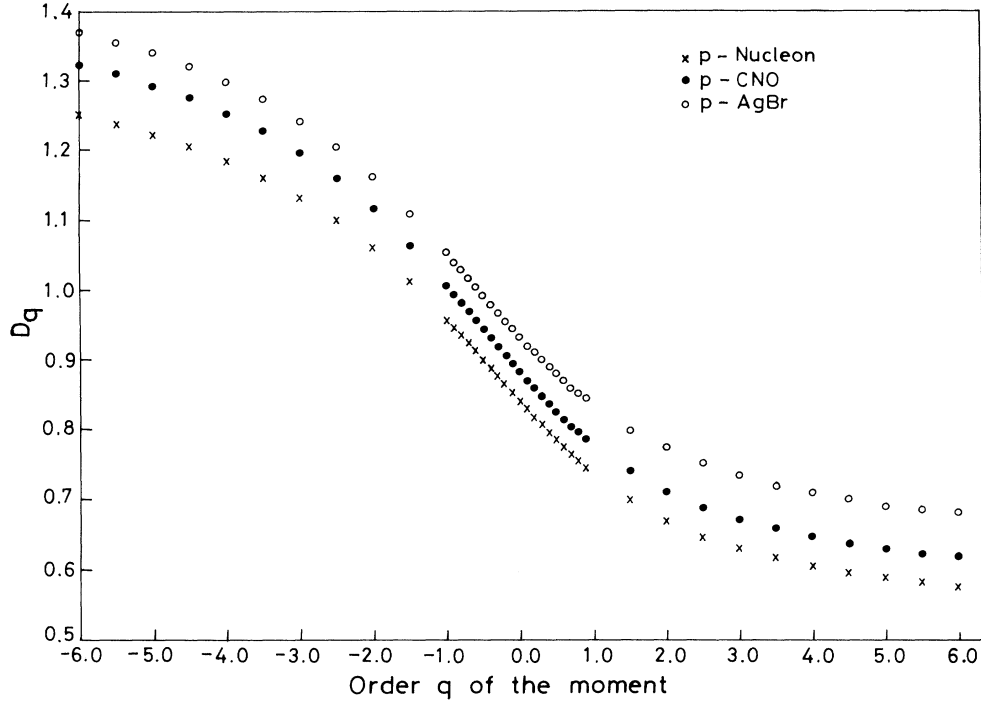


FIG. 9. The generalized dimensions (Renyi dimensions) D_q as a function of q (order of the moments) for p -nucleon interactions (\times), p -CNO interactions (\bullet), and p -AgBr interactions (\circ).

three ensemble of interactions and is plotted in Fig. 9 as a function of q , the order of the moments. For all the three types of interactions, the observed behavior of D_q with respect to q is in agreement with the multifractal cascade model [35]. As the target mass increases, $\langle N_s \rangle$ increases and hence the dimension D_q also increases.

Applying the theory of multifractals [23,26,27], we calculate the function [10] $f(\alpha_q)$ from $\langle Y(q) \rangle$ for a range of q using

$$\alpha_q = \frac{d}{dq} \langle Y(q) \rangle \quad (15)$$

and

$$f(\alpha_q) = q\alpha_q - \langle Y(q) \rangle. \quad (16)$$

Since a derivative is involved, hence $\langle Y(q) \rangle$ is determined for small incremental changes of q in the neighborhood of $q=0$, i.e., for $-1.0 < q < 1.0$, where $f(\alpha_q)$ has its maximum. So, α_q and $f(\alpha_q)$ are calculated for interactions with nucleon, CNO, and AgBr targets. Figure 10 shows the spectrum $f(\alpha_q)$ as a function of α_q for all the three cases. The entire spectrum $f(\alpha_q)$ contains far more information than the intermittency indices. The spectrum $f(\alpha_q)$ is concave for all the three cases centered at $\alpha_{q=0}$, which is compatible with the gluon model [11]. The peak of the spectrum $f(\alpha_q)$ is located at $\alpha_{q=0}=0.95$ (for nucleon targets), 0.99 (for CNO targets), and 1.04 (for AgBr targets). The left wing (for $q > 0$) of the spectrum $f(\alpha_q)$ describes the peaks and the right wing (for $q < 0$) of the spectrum $f(\alpha_q)$ describes the val-

leys of the single-particle pseudorapidity distribution [11] of the ensemble of events. The width of the spectrum describes the inhomogeneity of the pseudorapidity distribution. Thus the single-particle pseudorapidity distribution for nucleon interactions is more inhomogeneous than that for AgBr interactions, which is clearly observed in Fig. 1. The 45° line, drawn in Fig. 10 is tangent to the

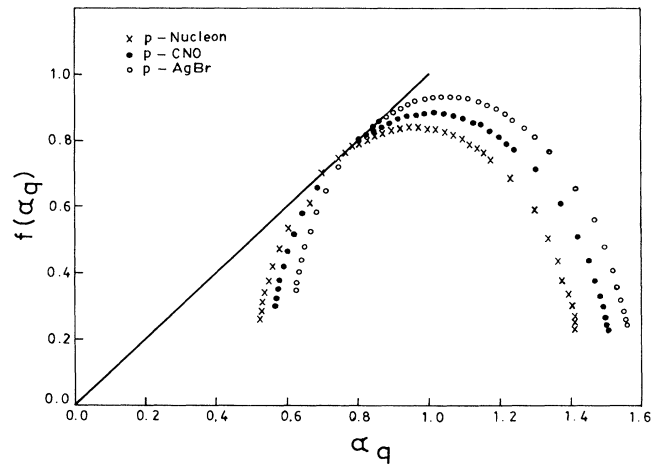


FIG. 10. The spectrum $f(\alpha_q)$ as a function of α_q for p -nucleon interactions (\times), p -CNO interactions (\bullet), and p -AgBr interactions (\circ).

TABLE IV. Values of various dimension (D_q) obtained from the spectrum $f(\alpha_q)$ [Eq. (16) in the text] for various targets. The errors are statistical.

Category	Fractal dimension $D_0=f(\alpha_0)$	Information dimension $D_1=f(\alpha_1)$	Correlation dimension $D_2=2\alpha_2-f(\alpha_2)$
p -nucleon	0.841 ± 0.058	0.700 ± 0.048	0.670 ± 0.046
p -CNO	0.883 ± 0.045	0.742 ± 0.037	0.713 ± 0.036
p -AgBr	0.932 ± 0.032	0.801 ± 0.027	0.773 ± 0.026

spectrum $f(\alpha_q)$ at $\alpha_{q=1}$ for all the three categories, which is a general property of the multifractals [11]. The maximum value of $f(\alpha_q)$ is for $q=0$ and it is $=0.84$, 0.88 , and 0.93 for interactions with nucleon, CNO, and AgBr targets, respectively. This implies that the number of empty bins is more in nucleon interactions and less in AgBr interactions for a range of $\delta\eta$ in which the self-similarity is observed. Thus, as the target mass increases, the peak value increases and shifts towards the higher value of α_q . The end points of the spectrum $f(\alpha_q)$, i.e., for $q=\pm\infty$ seems to be all positive, which can be interpreted as “no phase transition” in the α model [22]. The spectrum $f(\alpha_q)$ can be used in determining the fractal dimension $D_0=f(\alpha_0)$, the information dimension $D_1=f(\alpha_1)$ and the correlation dimension $D_2=2\alpha_2-f(\alpha_2)$ [13,24]. The values of these three dimensions is calculated and listed in Table IV for interactions with nucleon, CNO, and AgBr targets. The values of these three dimension are higher for AgBr interactions and lower for nucleon interactions. These three dimensions are sensitive to the production mechanism of the multiparticle production process [13]. The spectrum $f(\alpha_q)$ characterizes completely the dynamics of the particle production, as revealed in the multiplicity fluctuation.

From Eq. (11), it is clear that $G_1=1$ for all values of M and hence $\langle \ln G_1 \rangle = 0$ for all interactions, which is obvious from Eq. (13). Hence $\langle Y(1) \rangle = 0$ thus Eq. (16) yields $f(\alpha_1)=\alpha_1$. Hence at $q=1.0$, α_1 is the information di-

mension [13,24]. In order to sharpen the relationship among the various targets spectra, let us rescale the spectrum $f(\alpha_q)$ [28] as

$$\bar{\alpha}_q = \alpha_q / \alpha_1 \quad (17)$$

and

$$\bar{f}(\bar{\alpha}_q) = f(\alpha_q) / f(\alpha_1) = f(\alpha_q) / \alpha_1. \quad (18)$$

Figure 11 shows the rescaled spectrum $\bar{f}(\bar{\alpha}_q)$ for interactions with nucleon, CNO, and AgBr targets in which all the three curves coincide at $\bar{\alpha}_1 = \bar{f}(\bar{\alpha}_1) = 1$. All the three curves coincide for $\bar{\alpha}_q < 1$ and it is a form of universality for multifractal structure for $q > 1$. For $\bar{\alpha}_q > 1$ ($q < 1$), the universality holds between curves for nucleon and CNO interactions, but not for AgBr interactions. Thus, universality is obtained between the three curves for interactions with nucleon, CNO, and AgBr targets in the peaks of single-particle pseudorapidity distributions since the curves for $q > 1$ describe the peaks of the pseudorapidity distribution. In case of valleys of the pseudorapidity distribution, universality is found between nucleon and CNO interactions. When comparing the pseudorapidity distribution between the interactions with nucleon, CNO, and AgBr targets, it is concluded that the AgBr interactions have less valleys than those for nucleon and CNO interactions because the rescaled spectrum $\bar{f}(\bar{\alpha}_q)$ has less space in the $q < 1.0$ region. All the three rescaled curves are wide enough to resemble a multifractal multiplicity fluctuation and not a monofractal type.

V. CONCLUSION

We have studied the intermittency and multifractality for various targets namely, the nucleon, CNO, and AgBr targets in the emulsion experiment at 800 GeV.

From the study of intermittency, we conclude that an intermittent pattern is observed for all the three targets, which is more pronounced in nucleon interactions as compared to AgBr interactions. The observed pattern of anomalous fractal dimension d_q suggests that particle production is due to the self-similar cascade mechanism. The intermittent pattern is still obtained when the scaled factorial moment is corrected for the nonuniform shape of the pseudorapidity distribution and it is more pronounced in nucleon interactions compared to AgBr interactions. No evidence for phase transition is found even after the corrections.

From the multifractal analysis, we obtain more information on multiplicity fluctuation in the form of a smooth function $f(\alpha_q)$ than the intermittency. The

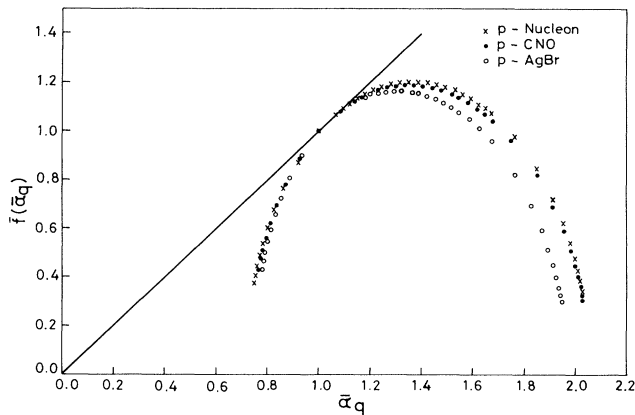


FIG. 11. The rescaled spectrum $\bar{f}(\bar{\alpha}_q)$ as a function of $\bar{\alpha}_q$ for p -nucleon interactions (\times), p -CNO interactions (\bullet), and p -AgBr interactions (\circ).

function $f(\alpha_q)$ leads to a better understanding about the peaks and valleys of the single-particle pseudorapidity distribution. If quarks and gluons are produced in the form of jets of particles by a cascade mechanism then the particles inside the jet show the self-similar behavior which leads to the fractal structure. Also, the more multifractal structure is pronounced, the more complex the collision and the higher the multiplicity. The multiplicity is an essential parameter which is related to the impact parameter of the collision. The spectrum $f(\alpha_q)$ also indicates that no phase transition is taking place in the interactions under study. The rescaled spectrum $\bar{f}(\bar{\alpha}_q)$ shows universality which is free from the complexity of the collision process in the region $\bar{\alpha}_q < 1$. The rescaled $\bar{f}(\bar{\alpha}_q)$ distributions are wide enough to signify that the

multiplicity fluctuation is multifractal and not monofractal.

Finally, we conclude that the multifractal analysis provides a better approach for studying and understanding the multiplicity fluctuations of multiparticle production than the intermittency.

ACKNOWLEDGMENTS

We are grateful to Fermi National Accelerator Laboratory, U.S., for exposure facilities at the Tevatron and to Dr. Ray Stefanski for help during exposure of the emulsion stack. We also thank Dr. R. Wilkes for processing facilities. One of us (V.K.V.) would like to acknowledge University Grants Commission, India for financial assistance.

-
- [1] W. Kittel, in *Proceedings of the Twentieth International Symposium on Multiparticle Dynamics*, Gut Holmecke, Germany, 1990, edited by R. Baier and D. Wegener (World Scientific, Singapore, 1991).
 - [2] For a recent review, see *Fluctuations and Fractal Structure*, Proceedings of the Ringberg Workshop on Multiparticle Production, Ringberg Castle, Germany, 1991, edited by R. C. Hwa, W. Ochs, and N. Schmitz (World Scientific, Singapore, 1992).
 - [3] B. Buschbeck and P. Lipa, *Mod. Phys. Lett. A* **4**, 1871 (1989).
 - [4] *Intermittency in High Energy Collisions*, Proceedings of the Santa Fe Workshop, Santa Fe, New Mexico, 1990, edited by F. Cooper, R. C. Hwa, and I. Sarcevic (World Scientific, Singapore, 1991).
 - [5] A. Bialas and R. Peschanski, *Nucl. Phys. B* **273**, 703 (1986); **B308**, 857 (1988).
 - [6] B. L. Hao, *Chaos* (World Scientific, Singapore, 1984).
 - [7] T. Sjostrand and M. Bengtsson, *Comput. Phys. Commun.* **43**, 367 (1987); T. Sjostrand, *Int. J. Mod. Phys. A* **3**, 751 (1988).
 - [8] T. Sjostrand, computer code JETSET 7.3, 1990.
 - [9] I. M. Dremin, *Mod. Phys. Lett. A* **3**, 1333 (1988); P. Lipa and B. Buschbeck, *Phys. Lett. B* **223**, 465 (1988); P. Carruthers, *Int. J. Mod. Phys. A* **4**, 5587 (1989).
 - [10] R. C. Hwa, *Phys. Rev. D* **41**, 1456 (1990).
 - [11] C. B. Chiu and R. C. Hwa, *Phys. Rev. D* **43**, 100 (1991).
 - [12] B. B. Mandelbrot, *The Fractal Geometry of Nature* (Freeman, New York, 1982); *J. Fluid Mech.* **62**, 331 (1974).
 - [13] R. C. Hwa, in *Quark Gluon Plasma*, edited by R. C. Hwa (World Scientific, Singapore, 1990).
 - [14] K. Sugano, in *Intermittency in High Energy Collisions* [4]; in *Proceedings of the Marburg Workshop on Correlations and Multiparticle Production*, Marburg, Germany, 1990, edited by M. Plümer, S. Raha, and R. Wiener (World Scientific, Singapore, 1991).
 - [15] UA1 Collaboration, H. Dibon and M. Markytan, in *Intermittency in High Energy Collisions* [4].
 - [16] CDF Collaboration, F. Rimondi, in *Proceedings of the Marburg Workshop on Correlations and Multiparticle Productions* [14].
 - [17] W. Kittel, in *Quark Gluon Plasma* [13].
 - [18] I. Derado, R. C. Hwa, G. Jancso, and N. Schmitz, *Phys. Lett. B* **283**, 151 (1992).
 - [19] I. Derado, J. Figiel, G. Jancso, and N. Schmitz, *Z. Phys. C* **54**, 357 (1992).
 - [20] N. Schmitz, in *Fluctuations and Fractal Structure* [2].
 - [21] K. Fialkowski, B. Wosiek, and J. Wosiek, *Acta Phys. Pol. B* **20**, 639 (1989).
 - [22] R. Peschanski, *Nucl. Phys. B* **327**, 144 (1989).
 - [23] G. Paladin and A. Vulpiani, *Phys. Rep.* **156**, 147 (1987).
 - [24] H. G. E. Hentschel and I. Procaccia, *Physica D* **8**, 435 (1983).
 - [25] P. Grassberger and I. Procaccia, *Physica D* **13**, 34 (1984).
 - [26] T. C. Halsey *et al.*, *Phys. Rev. A* **33**, 1141 (1986).
 - [27] T. C. Halsey and M. H. Jensen, *Physica D* **23**, 112 (1986).
 - [28] C. B. Chiu and R. C. Hwa, *Phys. Rev. D* **45**, 2276 (1992).
 - [29] C. Gupta, R. K. Shivpuri, N. S. Verma, and A. P. Sharma, *Phys. Rev. D* **26**, 2202 (1982).
 - [30] E. M. Friedlander, *Nuovo Cimento* **14**, 796 (1959); A. Barbaro-Galtieri *et al.*, *ibid* **21**, 469 (1961); B. Bhowmik and R. K. Shivpuri, *Phys. Rev.* **160**, 1227 (1967).
 - [31] A. Bialas and R. C. Hwa, *Phys. Lett. B* **253**, 436 (1991).
 - [32] A. Bialas and K. Zalewski, *Phys. Lett. B* **238**, 413 (1990).
 - [33] J. Feder, *Fractals* (Plenum, New York, 1988).
 - [34] R. C. Hwa, *Phys. Rev. D* **44**, 915 (1991).
 - [35] C. Meneveau and K. R. Sreenivasan, *Phys. Rev. Lett.* **59**, 1424 (1987).